Application of Radar Reflectivity Factor in Initializing Cloud-Resolving Mesoscale Model. Part I: Retrieval of Microphysical Elements and Vertical Velocity*

LIU Hongya[1,2†](刘红亚), XU Haiming[1](徐海明), HU Zhijin[2](胡志晋), XUE Jishan[2](薛纪善), and SHEN Tongli[1](沈桐立)

1 *Nanjing University of Information Science & Technology, Nanjing* 210044

2 *Chinese Academy of Meteorological Sciences, Beijing* 100081

(Received March 10, 2008)

ABSTRACT

Assuming that cloud reaches static state in the warm microphysical processes, water vapor mixing ratio ($q_{\rm v}$), cloud water mixing ratio ($q_{\rm c}$), and vertical velocity (w) can be calculated from rain water mixing ratio ($q_{\rm r}$). Through relation of Z-$q_{\rm r}$, $q_{\rm r}$ can be retrieved by radar reflectivity factor (Z). Retrieval results indicate that the distributions of mixing ratios of vapor, cloud, rain, and vertical velocity are consistent with radar images, and the three-dimensional spatial structure of the convective cloud is presented. Treating $q_{\rm v}$ saturated at the echo area, the retrieved $q_{\rm r}$ is about 0.1 g kg^{-1}, $q_{\rm c}$ is always less than 0.3 g kg^{-1}, w is usually below 0.5 m s^{-1}, and rain droplet terminal velocity ($v_{\rm r}$) is around 5.0 m s^{-1} in the place where radar reflectivity factor is about 25 dBz; in the place where echo is 45 dBz, the retrieved $q_{\rm r}$ and $q_{\rm c}$ are always about 3.0 g kg^{-1}, w is greater than 5.0 m s^{-1}, and $v_{\rm r}$ is around 7.0 m s^{-1}. In the vertical, the maximum updraft velocity is greater than 3.0 m s^{-1} at the height of around 5.0 km, the maximum cloud water content is about 3.0 g kg^{-1} above 5 km and the maximum rain water content is about 3.0 g kg^{-1} below 6 km. Due to the assumption that the cloud is in static state, there will be some errors in the retrieved variables within the clouds which are rapidly growing or dying-out, and in such cases, more sophisticated radar data control technique will help to improve the retrieval results.

Key words: radar, hydrometeors, nowcasting, cloud-resolving model

1. Introduction

The water phase transition and concomitant dynamic and thermal effects, generally called wet process, are very important to numerical weather prediction (NWP). Conventional observation is incapable of measuring mesoscale information and hydrometeors are not the direct observational elements. Thus hydrometeors are usually not analyzed in initial field but are created by model integration for a period of time. This causes the model precipitation behind the realization. With the development of high resolution numerical forecasting and observation techniques, as well as the progress of cloud-resolution model, especially with the increasing of radar and other indirect meteorological data, exploitation of indirect meteorological data is becoming a new direction of data assimilation technology (Chen and Xue, 2004).

Lin et al. (1993) developed the procedure of using radar data into initializing cloud-resolution model, and found that observation within 15 min is consistent with the prediction. Xue et al. (1998) utilized retrieved cloud water from radar reflectivity factor to the initial field and discovered a positive impact on the simulation of squall line. Guo et al. (1999) used radar data to change the humidity of initial field and ameliorated the prediction result of precipitation. Li et al. (2004a) made a prediction for 1 h with the cloud physical elements retrieved from radar reflectivity factor. Sheng et al. (2006) made experiments to compare the relative importance between assimilating radar data and increasing model resolution. Zhang et al. (2006) estimated wind using radar echo. However, other researches indicated that changing dynamic factors or

*Supported jointly by the National Natural Science Foundation of China under Grant Nos. 40233036 and 40305001 and the National Basic Research Program of China under Grant No. 2004CB418304.

†Corresponding author: red_asia@163.com.

thermodynamic factors of initial field separately could not make obvious improvement of prediction (Ninomiya and Kurihara, 1987).

Takano and Segam (1993) and Aonashi (1993) conducted experiments to enhance initial dynamical field and thermal field at the same time using radar data. Takano and Segam (1993) based on radar reflectivity factor to adjust the vertical profiles of temperature and humidity. Hu and Yan (1987) acquired initial hydrometeors by running model for a period of time under the condition of keeping dynamic field as constant, then used this initial field to restart model, improved rain prediction, and ameliorated the phenomena of precipitation lag at the early stage of prediction. But the applicability of the method entirely depended on the initial dynamic field. Sun and Crook (1997) developed a four-dimensional variational Doppler radar analysis system (4D-VDRAS). Xu et al. (2004) conducted numerical experiments using 4D-VDRAS. Li et al. (2004b) assimilated radar reflectivity factor by the relation with rain water mixing ratio adopted a three-dimensional variational technology. The advantage of variational methods lies on adopting nonlinear observational operators, extending the applicable field of observation. But these methods have rigid demands on operators while using tangent linear technology, whereas physical processes used in the variational method were largely simplified and could not describe the whole physical process. Because of the complexity in the method and its high computational cost, variational technologies are not irreplaceable in the operational application of radar data assimilation.

Physical variables of hydrometeors are main purposes of radar data retrieval. Precipitation not only is the main object of NWP but also plays an important role of direct feedback in atmosphere thermal, dynamical, and radiation processes via phase transform releasing latent heat, hydrometeor loading, and air density change (Liu and Hu, 2001; Liu et al., 2003; Lou et al., 2003). If only partial information of radar data is used, microphysical process may not match with dynamic process. For instance, while introducing hydrometeors based on observations into the descending domain of model, subsidence will be enhanced because of the evaporation of hydrometeors which leads to air cooling and cannot produce precipitation, then observations are rejected by model and even deteriorate model. Therefore, there are two important problems that the initialization of cloud-resolution model is facing, one is the initial value of cloud physical elements, and the other is the initial structure of mesoscale weather system. Retrieving-nudging method is used in this paper to initialize model. Cloud water, rain water, and vertical velocity retrieved by a one-dimensional steady model are used as the original value firstly, and then nudging technology is introduced to push this original value into a three-dimensional time-varying model. Eventually a physics-harmonious and observation-consistent atmospheric state is gained.

2. Water balance equations in cloud

Water exists in cloud in gaseous, liquid, and solid states. The liquid water can be further divided into cloud water ($q_{\rm c}$) and rain water ($q_{\rm r}$), and the solid water can be divided into ice crystal ($q_{\rm i}$), graupel ($q_{\rm g}$), snow ($q_{\rm s}$), hail ($q_{\rm h}$), etc. Water balance equations are generally written as the following (Sheng et al., 2003).

$$\frac{{\rm d}q_{\rm m}}{{\rm d}t} = \frac{1}{\rho}\frac{\partial}{\partial z}(\rho v_{\rm m} q_{\rm m}) + p_{\rm m} + Dq_{\rm m}, \quad (1)$$

where variable $q_{\rm m}$ is the mixing ratio of certain kind of hydrometeor in air, $v_{\rm m}$ is the mean terminal falling speed of hydrometeors, $p_{\rm m}$ is the transfer rate between different kinds of hydrometeors, ρ is air density, and z is height. On the right of Eq.(1), the first term is hydrometeor's drop term, the second is source/sink term, and the third is diffusion term. Drop term can be without consideration for cloud droplet and ice crystal and other small particles owing to their turbulence nature, raindrop and other larger particles can omit the diffusion term. Consequently, Eq. (1) can be rewritten as follows in Euler coordinates:

$$\frac{\partial q_{\rm m}}{\partial t} = -\boldsymbol{V}\cdot\nabla q_{\rm m} + \frac{1}{\rho}\frac{\partial}{\partial z}(\rho v_{\rm m} q_{\rm m}) + p_{\rm m} + Dq_{\rm m}. \quad (2)$$

The first term on the right of Eq.(2) called advection term, and $\boldsymbol{V}$ is a three-dimensional vector wind. For warm rain process without ice phase, equations of vapor ($q_{\rm v}$), cloud water ($q_{\rm c}$), and rain water ($q_{\rm r}$) can be written as

$$\frac{\partial q_{\rm v}}{\partial t} = -\boldsymbol{V}\cdot\nabla q_{\rm v} + P_{\rm RE} - P_{\rm CON} + Dq_{\rm v}, \quad (3)$$

$$\frac{\partial q_{\rm c}}{\partial t} = -\boldsymbol{V}\cdot\nabla q_{\rm c} + P_{\rm CON} - P_{\rm RC} - P_{\rm RA} + Dq_{\rm c}, \quad (4)$$

$$\frac{\partial q_{\rm r}}{\partial t} = -\boldsymbol{V}\cdot\nabla q_{\rm r} + \frac{1}{\rho}\frac{\partial}{\partial z}(\rho v_{\rm r} q_{\rm r}) + P_{\rm RC} + P_{\rm RA} - P_{\rm RE} + Dq_{\rm r}, \quad (5)$$

where $P_{\rm RE}$ is the rain evaporation rate in unsaturated air, $P_{\rm CON}$ is the condensation rate from vapor to cloud water, $P_{\rm RC}$ is the autoconversion rate from cloud water to rain water, $P_{\rm RA}$ is the accretion rate of cloud water by colliding rain, and $v_{\rm r}$ is the terminal falling velocity of raindrop. These terms are generally called microphysical conversion terms, positive or negative signs before these terms are used to identify the transition direction of hydrometeors, and the expressions of these terms are always gained by parameterization methods or microphysical schemes.

3. Microphysical parameterization process

Microphysical process is an important portion in cloud model. Given the spectra of condensation nuclei and hydrometeors and graded according to the size or quality standards, some empirical or statistical parameters are imported to express the conversion among hydrometeors and the interaction between microphysics processes and macrodynamic and thermal processes. According to warm rain scheme (Kessler, 1969), the autoconversion rate term, $P_{\rm RC}$, can be represented as

$$P_{\rm RC} = \begin{cases} \alpha(q_{\rm c} - q_{\rm crit}) & q_{\rm c} > q_{\rm crit} \\ 0 & q_{\rm c} < q_{\rm crit}. \end{cases} \quad (6)$$

The accretion rate term, $P_{\rm RA}$, is (Miller and Pearce, 1974)

$$P_{\rm RA} = \gamma q_{\rm c} q_{\rm r}^{7/8}. \quad (7)$$

The evaporation rate term, $P_{\rm RE}$, is (Kessler, 1969)

$$P_{\rm RE} = \beta(q_{\rm vs} - q_{\rm v})(\rho q_{\rm r})^{0.65}. \quad (8)$$

According to pseudo-adiabatic process, if liquid drops fall out of air parcel as soon as generated, the condensation rate term, $P_{\rm CON}$, can be written as

$$P_{\rm CON} = -\frac{{\rm d}q_{\rm vs}}{{\rm d}t} = -C\frac{{\rm d}p}{{\rm d}t} = -C\omega, \quad (9)$$

where C is a condensation function defined as (Tao and Xie, 1989)

$$C = -\frac{{\rm d}q_{\rm vs}}{{\rm d}p} = \frac{q_{\rm vs}T}{p}\Big(\frac{L_{\rm v}R - c_{\rm p}R_{\rm v}T}{c_{\rm p}R_{\rm v}T^2 + (q_{\rm vs}/1000.0)L_{\rm v}^2}\Big). \quad (10)$$

Hydrostatic relationship is assumed in background fields and based on the first order approximation of vertical movement equations, the relationship of vertical speed between p-coordinate (ω) and z-coordinate (w) can be written as

$$\omega = -\rho g w. \quad (11)$$

Substituting Eq.(11) into Eq.(9), we can derive

$$P_{\rm CON} = \rho g C w. \quad (12)$$

Saturation mixing ratio in Eq. (10) is given by (Sun et al., 1997)

$$q_{\rm vs} = \frac{380000}{p}\exp\Big[\frac{17.27(T - 273.16)}{T - 35.86}\Big]. \quad (13)$$

The unit of vapor mixing ratio, cloud water mixing ratio, and rain water mixing ratio is g kg^{-1}, and the unit of $P_{\rm RC}$, $P_{\rm RA}$, $P_{\rm RE}$, and $P_{\rm CON}$ is g kg^{-1} s^{-1}. The parameters mentioned above are as follows: α=0.001 s^{-1}, β=0.0486 s^{-1}, γ=0.002 s^{-1}, and $q_{\rm crit}$=1.5 g kg^{-1}. The latent heat of evaporation $L_{\rm v}$=2.5×10^6 J kg^{-1}. The unit of air density is kg m^{-3}, temperature (T) is K, pressure (p) is Pa, ω is Pa s^{-1}, w is m s^{-1}, condensation function (C) is g kg^{-1} Pa^{-1}, and gravity acceleration g=9.81 m s^{-2}. $c_{\rm p}$ is the specific capacity of air at constant pressure, here the specific capacity of dry air $c_{\rm pd}$= 1005 J kg^{-1} K^{-1} is adopted. Vapor constant $R_{\rm v}$=461.51 J kg^{-1} K^{-1}.

4. Derivation process of retrieval scheme

4.1 Relations between radar reflectivity factor and hydrometeors

Under the effect of gravity, the speed of a falling drop increases until the air resistance equals the pull of gravity quickly. As the drop continues to fall, it begins to fall at a constant speed, which is called terminal velocity. By definition, radar reflectivity factor and terminal velocity both have relations to the type of precipitation and the spectrum of hydrometeors. For the warm rain process only considering liquid water, where assuming a Marshall-Palmer drop-size distribution, the Z-$q_{\rm r}$ relation is (Sun et al., 1997)

$$Z = 43.1 + 17.5\log(\rho q_{\rm r}). \tag{14}$$

The $v_{\rm r}$-$q_{\rm r}$ relation is

$$v_{\rm r} = 5.40\alpha \cdot (\rho q_{\rm r})^{0.125}, \tag{15}$$

$$\alpha = (p_0/p)^{0.4}. \tag{16}$$

The unit of air density is kg m^{-3}, radar reflectivity factor (Z) dBz, rain water mixing ratio g kg^{-1}, basis pressure p and surface pressure p_0 Pa, and raindrop terminal velocity ($v_{\rm r}$) m s^{-1}.

Getting pressure (p) and temperature (T) from model forecast or observation firstly, air density can be calculated from the equation of state

$$\rho = p/RT, \tag{17}$$

where R is air constant, and the dry air constant $R_{\rm d}$=287.05 J kg^{-1} K^{-1} is adopted here. By rewriting Eq.(14), rain water mixing ratio can be gained from radar reflectivity factor in the form

$$q_{\rm r} = 10^{(Z-43.1)/17.5}/\rho, \tag{18}$$

and then the raindrop terminal velocity $v_{\rm r}$ can be calculated by substituting $q_{\rm r}$ into Eq.(15).

4.2 Simplification of water balance equation in warm rain process

Precipitation is a complex mutual influence process among dynamics, thermodynamics, and hydrometeors occurring in the atmosphere. When the physical properties of precipitation keep stable, variables do not change with time, which is called static state. Precipitation usually lasts for several hours or more than ten hours, in which its formation and dissipation phases take a relatively short time, and mature stage maintains for a long time and approximates a steady state. Hu et al. (1996) used the typical updraft distribution data which were observed from all kinds of rain bands occurring in extratropical cyclonic cloud systems, to calculate hydrometeors respectively with a one-dimensional model. Results indicated that the vertical distribution of precipitation flux at static state was consistent with observations in most situations. This demonstrated that the one-dimension static state hypothesis can reflect the real state of mature cloud properly. Therefore, under the assumption of static state, taking no account of turbulence and horizontal advection of cloud water and rain water, Eqs.(3), (4), and (5) can be rewritten as

$$\frac{\partial q_{\rm v}}{\partial t} = -\boldsymbol{V} \cdot \nabla q_{\rm v} + P_{\rm RE} - P_{\rm CON} = 0, \tag{19}$$

$$\frac{\partial q_{\rm c}}{\partial t} = -w\frac{\partial q_{\rm c}}{\partial z} + P_{\rm CON} - P_{\rm RC} - P_{\rm RA} = 0, \tag{20}$$

$$\frac{\partial q_{\rm r}}{\partial t} = -w\frac{\partial q_{\rm r}}{\partial z} + \frac{1}{\rho}\frac{\partial}{\partial z}(\rho v_{\rm r} q_{\rm r}) + P_{\rm RC} + P_{\rm RA} - P_{\rm RE} = 0. \tag{21}$$

If rain water falling fluxes decrease with increasing of height, then the air is assumed to be saturated in this level and no evaporation occurs, i.e., $P_{\rm RE}$=0. In this case, super-saturation is not permitted, and condensation occurs as soon as the air reaches saturation. From Eqs.(12) and (19), we obtain

$$\frac{{\rm d}q_{\rm v}}{{\rm d}t} = -P_{\rm CON} = -C\rho g w. \tag{22}$$

Adding Eqs.(20) to (21) and with the aid of Eq.(22), we can derive

$$w(\frac{\partial q_{\rm r}}{\partial z} + \frac{\partial q_{\rm c}}{\partial z} - \rho g C) = \frac{1}{\rho}\frac{\partial}{\partial z}(\rho v_{\rm r} q_{\rm r}), \tag{23}$$

namely

$$w = \frac{1}{\rho}\frac{\partial}{\partial z}(\rho v_{\rm r} q_{\rm r}) / \Big(\frac{\partial q_{\rm r}}{\partial z} + \frac{\partial q_{\rm c}}{\partial z} - \rho g C\Big). \tag{24}$$

Adding Eqs.(6) to (7), the term of $P_{\rm RC}$+$P_{\rm RA}$ can be written as

$$\begin{cases} P_{\rm RC} + P_{\rm RA} = \gamma q_{\rm r}^{0.875} q_{\rm c} & q_{\rm c} \leqslant q_{\rm crit} \\ P_{\rm RC} + P_{\rm RA} = (\gamma q_{\rm r}^{0.875} + \alpha) q_{\rm c} & \\ \qquad\qquad -\alpha q_{\rm crit} & q_{\rm c} > q_{\rm crit}. \end{cases} \tag{25}$$

Substituting Eq.(25) into Eq.(21) leads to

$$q_{\rm c}=\begin{cases}-\Big[\dfrac{1}{\rho}\dfrac{\partial}{\partial z}(\rho V_{\rm r}q_{\rm r})-w\dfrac{\partial q_{\rm r}}{\partial z}\Big]\\ \cdot(\gamma q_{\rm r}^{0.875})^{-1} & q_c\leqslant q_{\rm crit}\\ -\Big[\dfrac{1}{\rho}\dfrac{\partial}{\partial z}(\rho V_{\rm r}q_{\rm r})-w\dfrac{\partial q_{\rm r}}{\partial z}\\ -\alpha q_{\rm crit}\Big](\gamma q_{\rm r}^{0.875}+\alpha)^{-1}. & q_{\rm c}>q_{\rm crit}\end{cases}\quad(26)$$

Numerical solutions of vertical velocity (w) and cloud water mixing ratio ($q_{\rm c}$) can be gained by use of the iteration method from Eqs.(24) and (26).

The first and second terms in the denominator on the right side of Eq.(24) are far less than the third term, and thus we neglect the second term. $P_{\rm RC}$ is far less than $P_{\rm RA}$ and can also be omitted. Then, we can derive the directly solvable equations as below:

$$\begin{cases}q_{\rm v}=q_{\rm vs}\\ w=\dfrac{1}{\rho}\dfrac{\partial}{\partial z}(\rho v_{\rm r}q_{\rm r})/(\dfrac{\partial q_{\rm r}}{\partial z}-\rho gC)\\ q_{\rm c}=-[\dfrac{1}{\rho}\dfrac{\partial}{\partial z}(\rho v_{\rm r}q_{\rm r})-w\dfrac{\partial q_{\rm r}}{\partial z}]/(\gamma q_{\rm r}^{0.875}).\end{cases}\quad(27)$$

The solution of Eq.(27) can be used as the initial value of iteration method.

Now, under prerequisite that hydrostatic relation is satisfied in background fields, and precipitation remains a stationary state, ignoring horizontal advection and turbulence, and based on the warm rain process, we may extract the microphysical fields ($q_{\rm v}, q_{\rm c}, q_{\rm r}$) and dynamic field ($w$), using radar reflectivity factor data with the help of pressure and temperature in background fields. It should help to release the physical variables inconsistent problem, caused by only retrieving one of them, in the initial field of model to a certain extent.

5. Preprocessing of radar volume scan data

Calculation is convenient in the Cartesian coordinate system, and then it is needed to transform radar volume data into constant altitude levels. Mohr and Vaughan (1979) designed an economic coordinate transformation method; Zhou and Zhang (2002) and Liang et al. (2004) also did research in this area. The coordinate transformation and quality control method used in this paper will be described below based on the needs. The radar volume data employed in this paper are from "Research on the Formation Mechanism and Prediction Theory of Hazardous Weather of China", the National Natural Science Foundation of China (973 Project). This S-band Doppler weather radar situates at Hefei (31.867°N, 117.258°E), Anhui Province with an antenna altitude of 165 m. The resolution of reflectivity data in a radial direction is 1 km, the 14 elevations in vertical are: 0.5°, 1.5°, 2.4°, 3.4°, 4.3°, 5.3°, 6.2°, 7.5°, 8.7°, 10.0°, 12.0°, 14.0°, 16.7°, and 19.5°, with about 360 radial spacing approximately 1° apart on each level.

5.1 Coordinate transformation

Set radar horizontal situation on the sea level as the coordinate origin, x-axis pointing to east, y-axis pointing to north, and z-axis pointing upward, then

$$\begin{cases}x=r\cos\theta\sin\varphi\\ y=r\cos\theta\cos\varphi\\ z=h_0+r\sin\theta+0.375\times(r\cos\theta)^2/R_e,\end{cases}\quad(28)$$

where (x,y,z) is the grid point in the Cartesian coordinate system, (r,θ,φ) is the corresponding site (slant range, elevation, azimuth) in the spherical coordinate system, h_0 is the elevation of radar antenna, and the earth's radius $R_{\rm e}$=6378150 m.

5.2 Interpolation of radar reflectivity data

Giving the grid spacing (d) of every direction based on requirement, we can construct a cuboid gridding with the origin at radar antenna situation, and then fix the grid point $(x_{\rm o},y_{\rm o},z_{\rm o})$ gained by Eq.(28) on the gridding (i,j,k).

$$\begin{cases}i={\rm nint}(x_o/d+I_{\rm a}/2+1)\\ j={\rm nint}(y_o/d+J_{\rm a}/2+1)\\ k={\rm nint}[(z_o-h_0)/d],\end{cases}\quad(29)$$

where set d=500 m in every dimension, $I_{\rm a}$ and $J_{\rm a}$ are the total grid number of x-axis and y-axis, respectively, and "nint" means rounding off to the nearest integer.

The radar observation density and reliability decrease with the distance increasing both in horizontal and vertical directions, at the place 150 km away from the radar situation, the spacious resolution enlarges to about 4 km, thus, it is necessary to perform further smoothing process. In this paper, the average value of all points within horizontal 5-km and vertical 3-km ranges is taken as the value at central grid point of the cuboid.

5.3 Simple quality control

Quality control is necessary before the use of radar data. This paper mainly treats with the following points. Firstly, remove the isolated points in the horizontal directions. If the total number of observation point is less than 3 within 2 km of a point, then this point will be removed as a discrete observation. Secondly, get rid of clutter on levels near the ground. If there is no observation echo at a point on the level of 4 km above the antenna, but the corresponding point below 4-km levels has, then these data on low levels will be abandoned.

5.4 Results of the preprocessing

Figure 1 shows the reflectivity images on the 4-km level above radar antenna which are calculated through the method presented above, at 0201 BT 5 July 2003 at Hefei radar station. It can be seen that the two pictures are very similar. The contours are smoother on the picture gained by the technique of this paper, and weak echo at the rim of echo area is slightly enlarged due to taking the average of several points, but this will not influence the successive analysis, because we do not calculate cloud water content and vertical velocity at a point with echo intensity less than 20 dBz, and only set the vapor at this point to be saturated. We did not compare them on other levels because there is no image provided by radar station. The quality of processing result becomes worse at the place far away from radar site on account of the sparse observation, thus only the data below 10 km and within 150-km range from radar site are utilized in the subsequent retrieval and experiments.

6. Retrieval results

Figure 1 displays a typical precipitation echo containing stratus and cumulus on the Meiyu front, and there are several meso-γ cells embedded in a meso-β weather system. Based on the introduction of Zhang et al. (2001) to the Meiyu front precipitation echo, the echo whose density below 30 dBz is usually stratus, and there are always several cumulus, whose horizontal scale is about 5–30 km and echo density exceeds 40 dBz even beyond 50 dBz, spread on the broad stratus system. By the definition of Rutledge (1990), mesoscale convective system (MCS) means the precipitation weather system with a horizontal scale ranging from 100 to 500 km, live time at least several hours and generated prominent convective activities in its duration. In the different life stages of MCS, there is obvious change of the coverage of stratus and cumulus. In the initial stage, convective precipitation is at the dominating situation, the stratus area is usually as large as that of cumulus in a short time, and

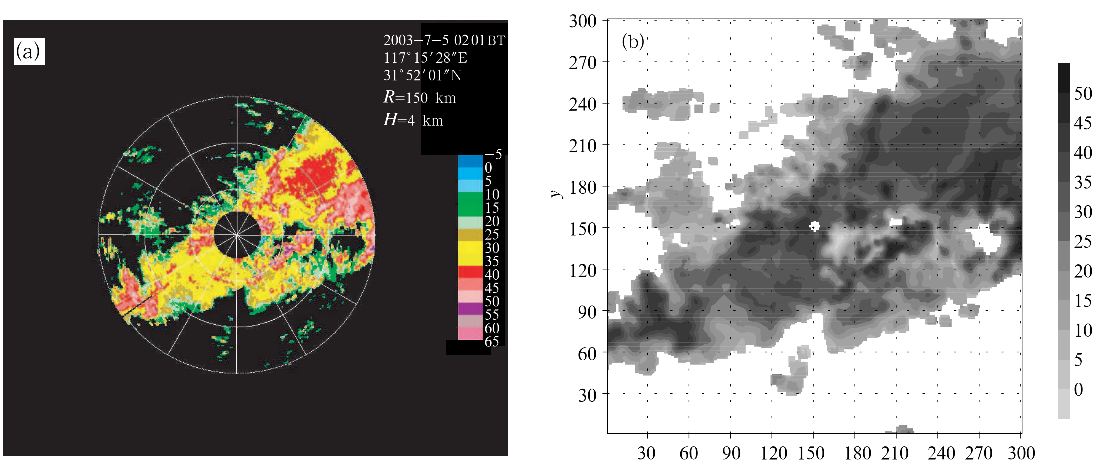

Fig.1. Comparison of 4-km height reflectivities (dBz) between (a) CAPPI image (range 150 km, Hefei radar, 0201 BT 5 July 2003) and (b) output treated by this paper's technique (grid spacing 1 km) at Hefei.

then at mature stage, stratus area always spreading three times cumulus coverage, finally, precipitation is mainly caused by stratus at the dying out stage. Therefore, the whole echo images in Fig.1 can be considered as an MCS.

In the following experiments, the echo area is set saturated, and calculation will not be made at the area where echo density below 20 dBz (no precipitation) or beyond 55 dBz (hail), retrieved results at 4-km height are shown in Fig.2. Comparing Figs.2b, c, e with Fig.1b, we can see that the spacial distributions of rain water, cloud water, and vertical velocity are consistent with radar echoes, and the magnitudes of variables increase quickly with intensification of echo. Cloud water and rain water have the same order of magnitude and below 0.5 g kg^{-1} in most areas, the maximum is about 3.0 g kg^{-1}, and therefore the superior limit of rain water is set as 5.0 g kg^{-1}. Ascending velocity in most areas is less than 0.3 m s^{-1}, the maximum is about 3.0 m s^{-1}, then the upper limit of vertical velocity is set as 5 m s^{-1}. Figure 2a indicates that the raindrop terminal velocity is rarely beyond 10.0 m s^{-1}, and the distribution of magnitude is according to echo density. Just as mentioned by McDonald (1958),

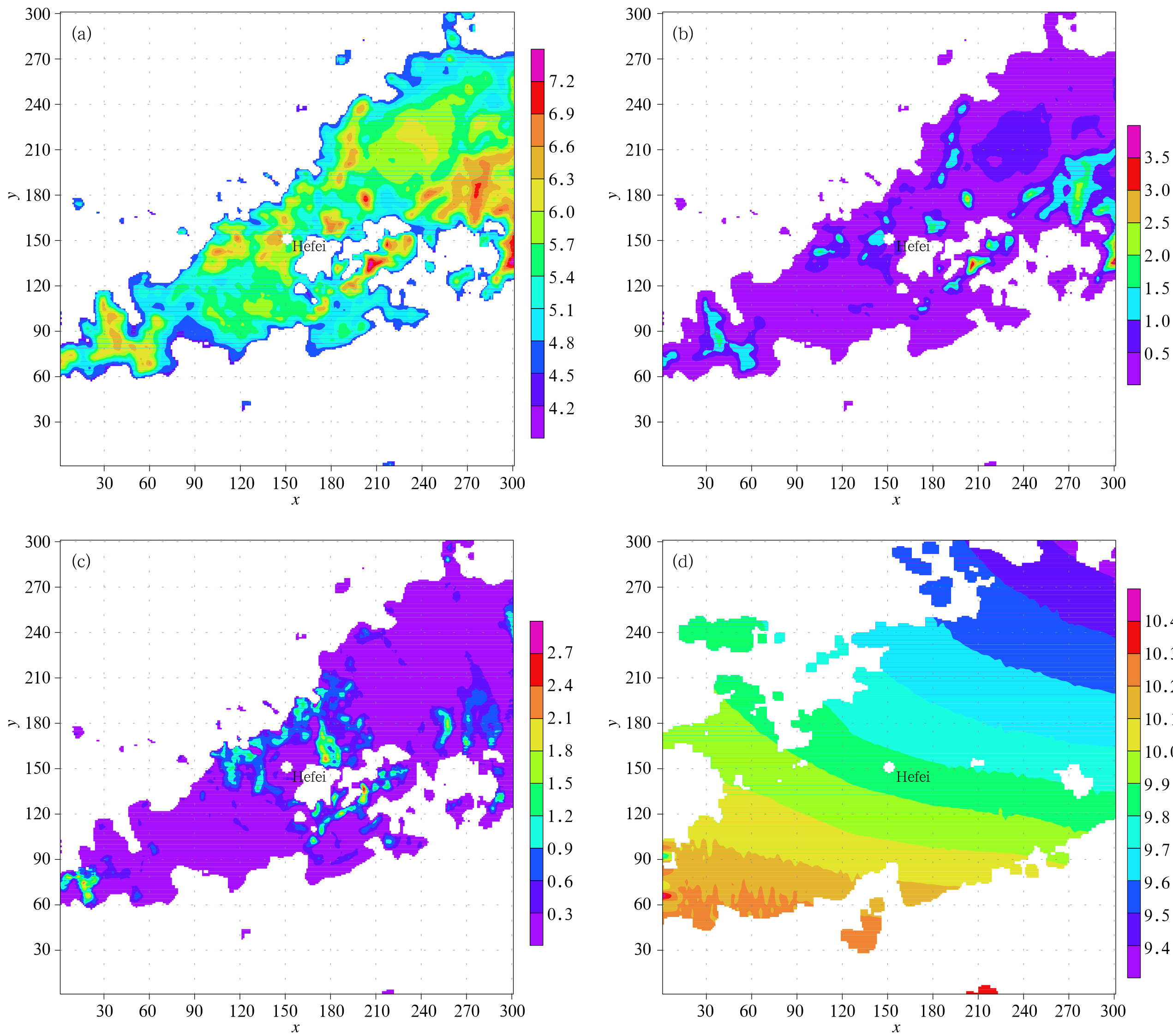

Fig.2. The 4-km height physical variable fields of (a) rain droplet terminal velocity and (e) air vertical velocity in m s^{-1}, and (b) rain water, (c) cloud water, and (d) water vapor mixing ratio in g kg^{-1}, at Hefei (grid spacing: 1 km).

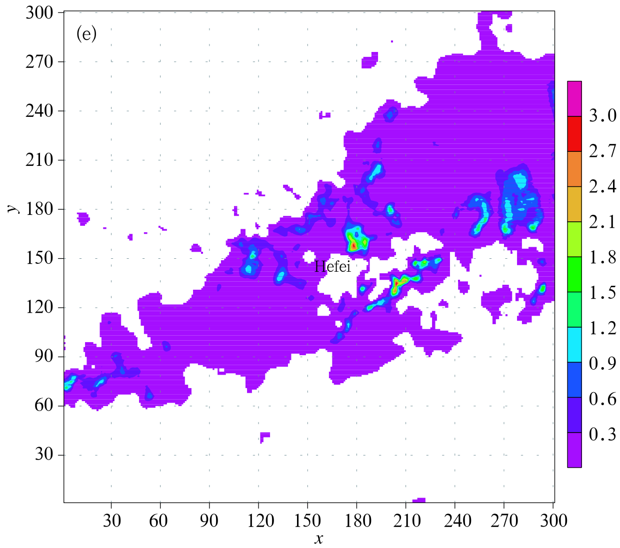

Fig.2. (Continued)

typical raindrop has a radius of about 1000 μm, number density is about 10^3 m^{-3} with the terminal velocity of 6.5 m s^{-1}. Figure 2d shows vapor field setting saturated. The analysis above indicates that the magnitudes of physical variables are rational, and the different characteristics between stratus and cumulus as depicted by Zhang et al. (2001) and Sheng et al. (2003) are as follows: The convective cloud is thick with intense ascendant current and the great water content inside, the average ascending velocity is several centimeters per second. The maximum upward speed can reach 20–30 m s^{-1} commonly in the middle of intensive convective cloud. Mean water content in convective cloud is about several grams per stere, with the maximum exceeding 10 g m^{-3}. Convective cloud top usually reaches 7–8 km, even stretches into the stratosphere. Convective cloud generally causes heavy precipitation, and the rainfall intensity can reach 20–30 mm h^{-1}, even beyond 50 mm h^{-1}. However, ascending speed in stratus is only several centimeters per second usually, and precipitation can last for more than several hours. Nimbostratus has a relatively bigger precipitation intensity and longer precipitation time among all kinds of stratus. The water content in stratus is close to adiabatic water content. It is generally one to two orders smaller than that of cumulus, about 10^{-2}–10^{-3} g m^{-3}. Stratus generally causes weak precipitation, about 0.7–2.7 mm h^{-1}.

The vertical distributions of physical variables are clearly displayed in Fig.3, showing that intensive echo area is mainly below 6 km, and the echo top is beyond the elevation of 10 km. The vertical structures of rain water, cloud water, vertical velocity, and raindrop terminal speed are consistent with that of radar echo. Because of temperature and pressure decrease with the increase of altitude, saturated vapor mixing ratio also reduces with height. Corresponding raindrop terminal velocity is about 5 m s^{-1}, rain water content is about 0.1 g kg^{-1} of the 25-dBz echo, the cloud water content generally below 0.3 g kg^{-1} with a higher situation opposite to rain water, and the vertical velocity is commonly not more than 0.5 m s^{-1}. To the echo whose intensity is 45 dBz, the corresponding raindrop terminal velocity is about 7 m s^{-1}, rain water content is about 3.0 g kg^{-1}, cloud water content also reaches 3.0 g kg^{-1} but at higher situation comparing to rain water, and ascending velocity even may reach 5 m s^{-1}. All these features are satisfied with the description about the Meiyu frontal torrential rain pattern by Zhang et al. (2001).

The vertical profiles of physical variables at one point in intensive echo areas, where convective activity is strong, are plotted in Fig.4. We can see that rain water is mainly located below 6 km and the maximum content occurs at the height of 4 km, ascending speed reaches peak at 5 km, cloud water mostly at the height above 5 km, raindrop terminal velocity only has slight alteration vertically with the maximum at 5 km. These characteristics verify that this is a Meiyu frontal heavy rain, not a severe storm system, because the height of extensive echo and existing maximum in negative temperature area in cloud are the major factors to distinguish heavy precipitation thunderstorm and hail-causing thunderstorm. In the Meiyu frontal cloud system, intensive echo area is located below 0°C height and echo intensity rapidly reduces with the increase of height above 0°C level, indicating big raindrops are mainly concentrated in warm domain below the height of 0 °C and precipitation is chiefly caused through coagulation process. The moderate ascending velocity in cumulonimbus in Meiyu front usually does not exceed 3 m s^{-1} (Zhang et al., 2001).

The above analyses indicate that the spacial distributions of physical factors retrieved in this paper accord with radar echoes and their magnitudes are rational, and displayed the features of Meiyu frontal precipitation, the distinctions between cumulus and stratus are very clear. Especially to convective cloud whose echo intensity greater than 35 dBz, cloud microphysical elements and vertical velocity are coordinated quite well both in magnitude and position. The retrieval results must pass through further processing before used as initial state, because they still do not match with the horizontal winds, temperature, and pressure in the initial field. Nudging technique is adopted to carry out this task, and the details and related experiment results are presented by Liu et al. (2007).

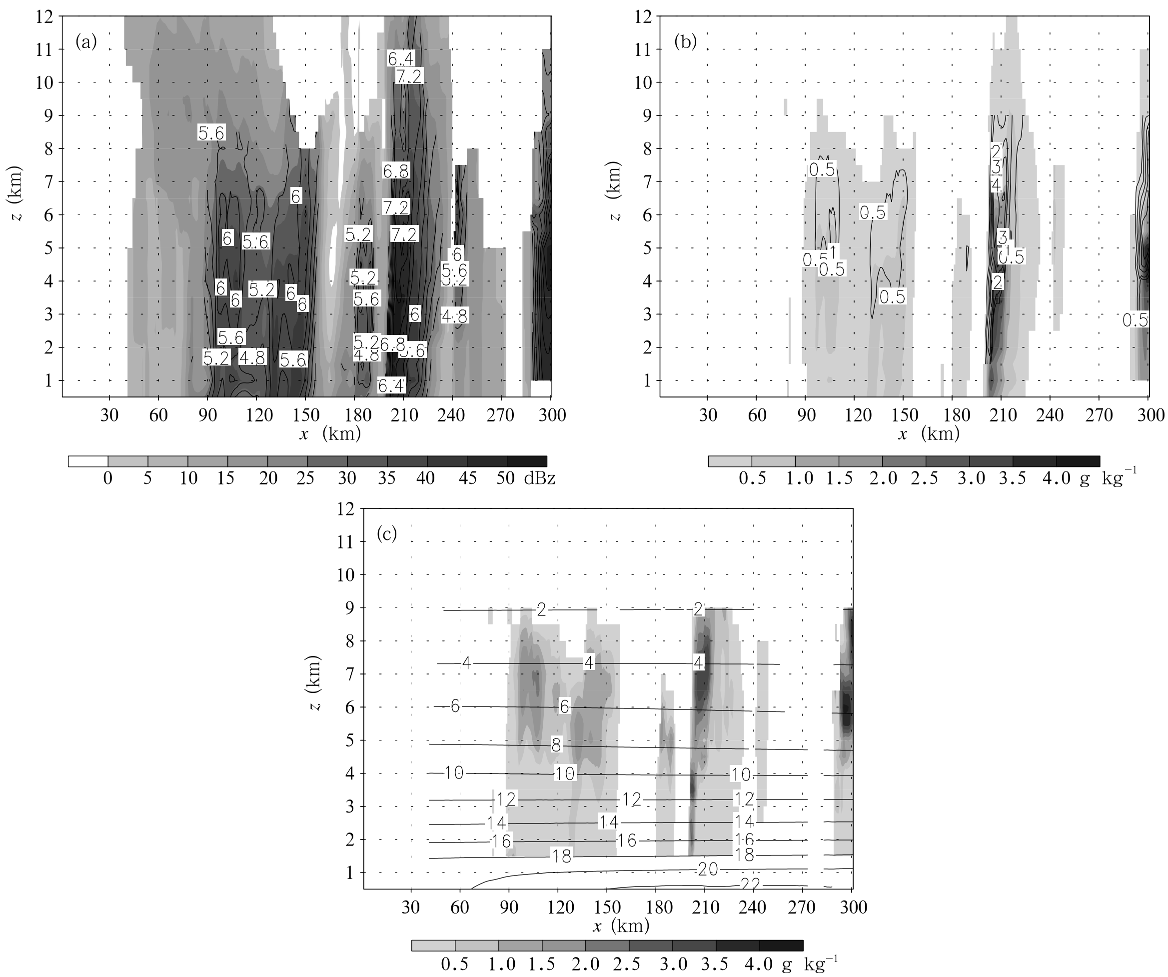

Fig.3. $x-z$ cross section of (a) reflectivity (shading; dBz) and raindrop terminal velocity (contours; m s^{-1}), (b) rain mixing ratio (shading; g kg^{-1}) and vertical velocity (contours; m s^{-1}), and (c) cloud water (shadings) and water vapor (contours) mixing ratio (g kg^{-1}) along y=135 (grid spacing: 1 km).

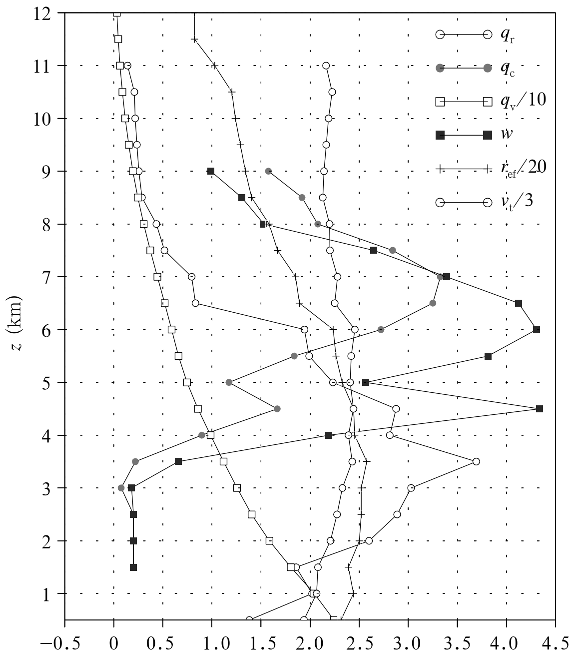

Fig.4. Vertical profiles of various physical variables (units are the same as Fig.3) at grid-point (208, 135).

7. Discussion and conclusion

The processing of radar observations and the retrieval technique of vapor, cloud water, rain water, and vertical velocity were presented in this paper. The comparison results at 4-km height indicate that the radar data processing method developed in this paper is available within the radius of 150 km centered at radar cite. The magnitudes of retrieval of hydrometeors and vertical velocity are reasonable, and the spacial distributions are consistent with the radar echo and compatible each other. The main features of heavy rain occurring on Meiyu front are exhibited obviously, and there are notable differences between stratus and cumulus. Retrieval schemes are developed under the assumption that precipitation keeps constant, which could bring errors when used in growing period or dissipating stage. Furthermore, the density of observation has important impact on the quality of retrieval results, the cone areal above radar is disadvantage for data lacking at this area, the place far away from radar should lead to very big values of cloud water and vertical speed when derivating with respect to height because of the sparse observation. The joint utilization of neighboring radars' data will help to mend the deficient of data.

REFERENCES

Aonashi, K., 1993: An initialization method to incorporate precipitation data into a mesoscale numerical weather prediction model. *J. Meteor. Soc.*, **71**(3), 393–406.

Chen Dehui and Xue Jishan, 2004: An overview on recent progresses of the operational numerical weather prediction models. *Acta Meteorologica Sinica*, **62**(5), 621–633. (in Chinese)

Guo Xia, Dang Renqing, and Ge Wenzhong, 1999: the use of radar data in the numerical simulation of heavy rainfalls in the Changjiang-Huaihe River basin. *Journal of Tropical Meteorology*, **15(**4), 356–362. (in Chinese)

Haase, G., S. Crewell, C. Simmer, and W. Wergen, 2000: Assimilation of radar data in mesoscale models: Physical initialization and latent heat nudging. *Phys. Chem. Earth(B)*, **25**,1237–1242.

Hu Zhijin and Yan Caifan, 1987: Numerical simulation of microphysical processes of stratiform clouds. (Π): Microphysical processes in middle latitude cyclone cloud systems. *Journal of Applied Meteorological Science*, **2**(2), 133–142. (in Chinese)

Hu Zhijin, Liu Songbo, and Zhu Tong, 1996: Research of cloud scheme of heavy rain numerical prediction. *Operational Nemerical Prediction Method and Technology Research on Typhoon Rainstorm.* Pang Jinbo, Eds. China Meteorological Press, Beijing, 593–602. (in Chinese)

Kessler, E., 1969: On the distribution and continuity of water substance in atmospheric circulation. *Meteor. Monogr.*, **32**, 1–84.

Li Yongping, Yuan Zhaohong, and Wang Xiaofeng, 2004a: Microphysical adjustments using reflectivity of Doppler radar for mesoscale model. *Journal of Applied Meteorological Science*, **15**(6), 658–664. (in Chinese)

Li Yongping, Zhu Guofu, and Xue Jishan, 2004b: Microphysical retrieval from Doppler radar reflectivity using variational data assimilation. *Acta Meteor. Sinica*, **62**(6), 814–820. (in Chinese)

Liang Haihe, Ruan Zheng, and Ge Runsheng, 2004: HUAMEX radar data processing method. *Journal of Applied Meteorological Science*, **15**(3), 281–290. (in Chinese)

Lin Y. P., P. S. Ray, and K. W. Johnson, 1993: Initialization of a modeled convective storm using Doppler radar derived fields. *Mon. Wea. Rev.*, **121**, 2757–2775.

Liu Hongya, Xu Haiming, Xue Jishan, Hu Zhijin, and Shen Tongli, 2007: Radar reflectivity factor applied to initialize cloud-resolving mesoscale model. Part Π: Numerical simulation experiment. *Acta Meteor. Sinica*, **22**

Liu Qijun and Hu Zhijin, 2001: Wet physical process and physical initialization method of mesoscale model. *Meteorological Science and Technology*, **29**(2), 1–10. (in Chinese)

Liu Qijun, Hu Zhijin, and Zhou Xiuji, 2003: Explicit cloud schemes of HALFS and simulation of heavy rainfall and clouds. Part I: Explicit cloud schemes. *Journal of Applied Meteorological Science*, **14**(supplement), 60–67. (in Chinese)

Lou Xiaofeng, Hu Zhijin, Wang Pengyun, and Zhou Xiuji, 2003: Introduction to microphysical schemes of mesoscale atmospheric models and cloud models. *Journal of Applied Meteorological Science*, **14**(supplement), 19–59. (in Chinese)

McDonald, J. E., 1958: The physics of cloud modification. *Advances in Geophysics*, **5**, 223–303.

Miller, M. J., and R. P. Pearce, 1974: A three-dimensional primitive equation model of cumulonimbus convection. *Quart. J. Roy. Meteor. Soc.*, **100**, 133–154.

Mohr, C. G., and R. L. Vaughan, 1979: An economical procedure for Cartesian interpolation and display of reflectivity factor data in three-dimensional space. *Appl. Meteor.*, **18**, 661–670.

Ninomiya, K., and K. Kurihara, 1987: Forecast experiment of a long-lived meso-α-scale convective system in Baiu front zone. *J. Meteor. Soc. Jap.*, **65**, 885–899.

Sheng Chuanyan, Xue Deqiang, Lei Ting, and Gao Shouting, 2006: Comparative experiments between effects of Doppler radar data assimilation and increasing horizontal resolution on short-range prediction. *Acta Meteor. Sinica*, **64**(3), 293–307. (in Chinese)

Sheng Peixuan, Mao Jietai, Li Jianguo, Zhang Aichen, Sang Jianguo, and Pan Naixian, 2003: *Atmospheric Pysics*. China Meteorological Press, Beijing, 522 pp. (in Chinese)

Sun J., and N. A. Crook, 1997: Dynamical and microphysical retrieval from Doppler radar observations using a cloud model and its adjoint. Part I: Model development and simulated data experiments. *J. Atmos. Sci.*, **54**, 1642–1661.

Steven, A. Rutledge, Chungu Lu, and Donald R. Macaorman, 1990: Positive cloud-to-ground lighting in mesoscale convective systems. *Journal of the Atmospheric Sciences*, **47**(17), 2085–2100.

Takano, I., and I. A. Segam, 1993: Assimilation and initialization of a mesoscale model for improved spin-up of precipitation. *J. Meteor. Soc. Jap.*, **71**, 377–391.

Tao Zuyu and Xie An, 1989: *Weather Process Diagnostic Analysis Principle and Practice*. Peking University Press, Beijing, 215 pp. (in Chinese)

Xu Xiaoyong, Zheng Guoguang, and Liu Liping, 2004: Dynamical and microphysical retrieval from simulated Doppler radar observations using the 4DVAR assimilation technique. *Acta Meteor. Sinica*, **62**(4), 410–422. (in Chinese)

Xue M., Wang D., Hou D., K. Brewster, and K. K. Droegemeier, 1998: Prediction of the 7 May 1995 squall line over the central U. S. with intermittent data assimilation. 12th Conf. on Numerical Weather Prediction. Phoenix, Arizona, Amer. Meteor. Soc., 191–194.

Zhang Peichang, Du Bingyu, and Dai Tiepi, 2001: *Radar Meteorology*. China Meteorological Press, 511 pp. (in Chinese)

Zhang Yaping, Cheng Minghu, Xia Wenmei, Cui Zhehu, and Yang Hongping, 2006: Estimation of weather radar echo motion field and its application to precipitation nowcasting. *Acta Meteor. Sinica*, **64**(5), 631–646. (in Chinese)

Zhou Haiguang and Zhang Peiyuan, 2002: A new technique of recovering three-dimensional wind fields from simulated dual-Dopler radar data in the Cartesian space. *Acta Meteor. Sinica*, **60**(5), 585–193. (in Chinese)